

Article

# Pneumatic Multi-Pocket Elastomer Actuators for Metacarpophalangeal Joint Flexion and Abduction-Adduction

Tapio Veli Juhani Tarvainen <sup>1</sup> and Wenwei Yu <sup>1,2,\*</sup>

<sup>1</sup> Department of Medical Engineering, Graduate school of Engineering, Chiba University, Inage-ku, Yayoi-cho, 1-33, Chiba 263-8522, Japan; tapio.tarvainen@chiba-u.jp

<sup>2</sup> Center for Frontier Medical Engineering, Chiba University, Inage-ku, Yayoi-cho, 1-33, Chiba 263-8522, Japan

\* Correspondence: yuwill@faculty.chiba-u.jp; Tel.: +81-43-290-3231

Received: 22 July 2017; Accepted: 6 September 2017; Published: 19 September 2017

**Abstract:** During recent years, interest has been rising towards developing fluidic fiber-reinforced elastomer actuators for wearable soft robotics used in hand rehabilitation and power-assist. However, they do not enable finger abduction-adduction, which plays an important role in activities of daily living, when grasping larger objects. Furthermore, the developed gloves often do not have separate control of joints, which is important for doing various common rehabilitation motions. The main obstacle for the development of a fully-assisting glove is moving a joint with multiple degrees of freedom. If the functions are built into the same structure, they are naturally coupled and affect each other, which makes them more difficult to design and complex to control than a simple flexion-extension actuator. In this study, we explored the key design elements and fabrication of pneumatic multi-pocket elastomer actuators for a soft rehabilitation glove. The goal was to gain more control over the metacarpophalangeal joint's response by increasing the degree of actuation. Three main functional designs were tested for achieving both flexion and abduction-adduction. Five prototypes, with four different actuator geometries and four different reinforcement types, were designed and fabricated. They were evaluated by recording their free motion with motion capture and measuring their torque output using a dummy finger. Results showed the strengths and weaknesses of each design in separating the control of the two functions. We discuss the different improvements that are needed in order to make each design plausible for developing an actuator that meets the requirements for full assist of the hand's motions. In conclusion, we show that it is possible to produce multi-pocket actuators for assisting MCP joint motion in both flexion and abduction-adduction, although coupling between the separate functions is still problematic and should be considered further.

**Keywords:** soft robotics; fluidic elastomer actuators; fiber-reinforced; multi-pocket; hand rehabilitation; finger abduction-adduction

---

## 1. Introduction

### 1.1. Background

The probability of stroke, physical trauma and disease-related disabilities increases with age, as the body becomes more fragile. Thus, as the population ages in developed countries, demand for rehabilitation therapy increases to support the people in remaining as functioning members of society. This has led to increased interest towards developing devices that could be used for supporting, protecting and recovering the functions of the aging human body [1–4].

Previous studies have shown that using robotic systems may improve the quality and outcome of rehabilitation and ease the increasing workload of therapists [4]. However, traditionally, these devices

have been based on rigid mechanics, which requires precision engineering to ensure safe forces and torques on the joints [5]. This safety concern leads to high cost, which is one of the main obstacles for introducing new clinical products [3]. Furthermore, effective rehabilitation often requires exercises to be done at home. This leads to the need for easy-to-use portable low-cost devices [3]. Thus, there is room for developing completely different approaches.

Soft robotics research concentrates on developing highly compliant structures for a wide variety of applications [6]. Recent advances in the field have brought new methods for developing light and safe wearable devices that can be used for power-assist and rehabilitation [7–10]. These structures can be used for coupling the forces from actuators to the human body safely and efficiently, because they conform to its shape and follow its natural joint trajectories, although with some safety precautions [5]. Furthermore, the materials and methods for making soft robotics are often much lighter and less expensive than those used for making equivalent rigid mechanisms. Especially hand rehabilitation is a field where soft wearable devices could prove useful, as they have the potential to support the hand motions, without blocking or otherwise hindering them, while being light and comfortable to wear.

Hand rehabilitation exercises are done to recover lost functions by mobilizing and activating as many of the joints and muscles of the hand as possible. This reduces muscle and joint stiffness, minimizes loss of muscle and bone mass and prevents the possible formation of scar tissue [11]. These hand exercises are often referred to as six-pack, meaning six simple mobilizing exercises, which include (with some variation depending on the therapist):

1. Flexion-extension of finger Metacarpophalangeal (MCP) and thumb carpometacarpal joints
2. Flexion-extension of Interphalangeal (IP) joints to form a hook
3. Flexion-extension of MCP and proximal IP joints
4. Forming a fist
5. Finger and thumb abduction-adduction
6. Thumb opposition to each finger and sliding thumb from the tip of little finger to its base

## 1.2. Related Research

Several groups around the world have started to develop soft hand rehabilitation and power-assist systems [12–14]. These systems are based on soft fluidic fiber-reinforced actuators, which consist of a pneumatically- or hydraulically-pressureized pocket, or chamber, enclosed in a polymer, which is reinforced with soft strain limiting materials.

There have been several studies on different designs for this type of actuator. Gerboni et al. [15] developed modular soft manipulators with multi-pocket structures for minimally-invasive surgery; Park et al. [9] prototyped a power-assist device for the knee; Deimel and Brock [16] used them as fingers for their robotic hand; and finally, Noritsugu et al. [12], Polygerinos et al. [13] and Yap et al. [14] each developed their own versions of a portable power-assist/rehabilitation glove.

The current soft fluidic actuators for rehabilitation and power-assist glove systems control only one axis of motion for each joint [12–14]. This means that the motion of the MCP joint can be supported only in one degree of freedom (DoF), although it has two, flexion-extension and abduction-adduction. So far, the final prototypes of the developed systems have assisted each finger only in flexion-extension and have not included the abduction-adduction motion [12–14], which is an important function in activities of daily living, as it enables grasping of larger objects. Therefore, the current designs do not achieve a full set of six-pack exercise motions. Furthermore, as the actuators have only one input, these systems cannot control the joints separately. Instead, several actuators need to be attached [12], which leads to cluttering of input tubing, or the actuators need to be switched according to the exercise [17], which makes the device less convenient to use, for example in an at-home rehabilitation scenario.

A major obstacle for implementing a full 2-DoF support for the MCP joint may be the coupling of the DoFs, when this type of actuator used. The two designed functions may conflict and affect each

other, which makes it difficult to control motion only in one direction. In other words, combining flexion and abduction-adduction functions in one actuator may, e.g., cause it to flex forward, when only abduction is intended.

### 1.3. Goals of This Study

Our final goal is to make a power-assist glove that can be used for assisting all six-pack exercises. In our present study, we have concentrated on exploring the design of soft actuators for achieving full assist of the MCP joint motions, including both abduction-adduction and flexion-extension. We have excluded the distal joints of the fingers from this consideration, as they have only a single DoF, and achieving the flexion-extension motion has been studied extensively before [12–14,18].

By adding separately-controlled pockets to the actuators, i.e., increasing the number of degrees of actuation (DoA), it could be possible to control the motion of each joint separately, also including the abduction-adduction motion, and achieving all six-pack exercises. However, we need to solve the problem of coupling between the two DoFs, while meeting the functional requirements for each of them, to make this approach plausible.

The main focus of this manuscript is to describe and evaluate the feasibility of three functional designs for multi-pocket actuators for 2-DoF MCP joint motion assist. The description of our study is divided into two parts. In the first part, we explain the design principles and design of our actuators, and in the second, we describe the fabrication and evaluation of the prototypes.

## 2. Actuator Prototype Design

In this section, we describe the basic design principles we used for our actuators, their functional requirements and the different prototype designs that we fabricated and evaluated.

### 2.1. Design Principles

The function of a fluidic elastomer actuator is defined by the expansion properties of its structure, when its internal pressure is changed. In other words, it is a balloon that has been restricted from expanding in specific parts, which makes it exert forces and achieve motions and functions in desired directions.

The direction and strength of the actuator's expansion are controlled by four principles:

1. Geometry of the elastomer structure;
2. Heterogeneity of elastomer materials used;
3. Material properties and geometry of embedded reinforcing and strain-limiting materials;
4. Coupling between the actuator and the moved object or structure.

Controlling the expansion by adjusting the geometry of an otherwise homogeneous material is perhaps the simplest approach. The basic principle is that thinner walls will deform more than thicker ones, when the actuator is pressurized. This is due to the relative difference in stiffness of the walls. Furthermore, the alignment of separately-expanding pockets relative to each other has a major influence on the actuator's response, as the passive pockets still affect the expansion of the active pockets through the surrounding structures. For simple geometries, it is possible to estimate the deformation by using basic beam equations [16,19]. However, the finite element method is often used in simulation studies for estimating the response of more complex geometries [20]. The effects of changing different structural parameters, such as wall thickness, have been considered in several previous studies, e.g., by Deimel and Brock [16], Polygerinos et al. [20] and Udupa et al. [21].

The second principle is to have different types of elastomers arranged in the actuator body so that the ones with higher stiffness work as strain limiters for the more elastic ones. Again, the stiffness parameter defines which parts of the actuator deform the most relative to the other parts. An example of this is the study on finger-like actuators by Connolly et al. [22]. However, in our study, we use only one type of silicone elastomer to reduce the number of variables affecting the actuators' response.

Instead of using heterogeneous elastomers, it is also possible to change the relative stiffness by embedding, or laminating, pre-made structures into the elastomer that forms the main body of the actuator. These structures can be for example in the form of a sheet or net that partially or completely limits the strain of the side of the actuator on which it is placed [16,20]. Another commonly-used structure is a reinforcement fiber that is wound around the actuator in specific patterns and angles, limiting the radial expansion and, for example, causing the actuator to twist around its longitudinal axis [23]. Combining actuators in parallel with different patterns of reinforcement fibers has also been tested by Bishop-Moser et al. [24].

Finally, the method of coupling the actuator to the object it moves, e.g., a finger, defines the last restrictions for its expansion. The different straps and sleeves that are used for the connection restrict the actuator's expansion [25], while the shape and mobility of the finger add further constraints to its motion.

## 2.2. Functional Requirements

In this study, we concentrated only on the motion assist of the finger MCP joint, as the flexion of the distal joints has been studied in depth in previous studies, and we have already developed our methods for including those joints in a full finger actuator [18].

Our main goal was to develop actuators to control the two-directional motion of the MCP joint easily and efficiently. Thus, the main requirement was the ability of actuators to control these two DoFs separately, or in other words, minimizing the detrimental effects between the two functions built into the same structure.

In order to have full motion assistance of the MCP joint, the actuators need to have a wide enough Range of Motion (RoM). As a reference for this, we used the full active RoMs for the finger MCP joints. They are on average:  $-45^\circ$ – $100^\circ$  for flexion-extension and  $-20^\circ$ – $20^\circ$  for abduction-adduction [26,27]. We did not consider extension in this study, but had it only as a passive function through material stiffness. Thus, we set the target flexion-extension RoM to be  $0^\circ$ – $100^\circ$ . The actuators also need to expand in length in order to compensate for the length difference between the top of a straight and bent joint. In the prototype design, this property was only approximated, as it was not the main focus of our study.

Further, the actuators need to transfer enough torque to the joint to make it move. The torque requirements are naturally different for a relaxed hand and a hand that is suffering from joint stiffness caused by either scar tissues, or possible muscle spasticity related to neurological impairments. We approximated this requirement based on acceptable torques for assisting the index finger MCP joint motions. They are approximately 24–30 Ncm for flexion-extension and 17 Ncm for abduction-adduction, according to a previous assessment by Kawasaki et al. [28].

Finally, the actuators need to be reliable and safe [5]. Thus, they should have a precise and accurate enough output, which should not change radically during use. Furthermore, they should be robust to not get damaged easily and have a low pressure to torque output ratio, to mitigate dangers, if they do get damaged.

Considering these requirements and applying the four design principles, we produced the following three main functional designs.

## 2.3. General Prototype Design Specifications

All of the designed actuators had the same basic dimensions (Figure 1), approximated to match the size of an average index, middle or ring finger, based on measurements by Buryanov et al. [29].

The root part had a connector groove for connecting the actuators to a test bench or a supporting orthotic structure on the hand. All pressure input tubing was inserted through the root part into the pockets. Each prototype had ready guide grooves around it for a radially-reinforcing string. These grooves were set to be at 2-mm intervals along the actuator.

Overall, four different internal geometries (Simple1, Simple2, Opposing and Parallel) and four different reinforcement types (A–D) were designed for five prototypes (Simple1-A, Simple2-A, Simple2-B, Opposing-C, and Parallel-D). Details of the differences in the prototypes' geometry and reinforcements are shown in Figures 1 and 2, respectively. These details are described further in the following sections.

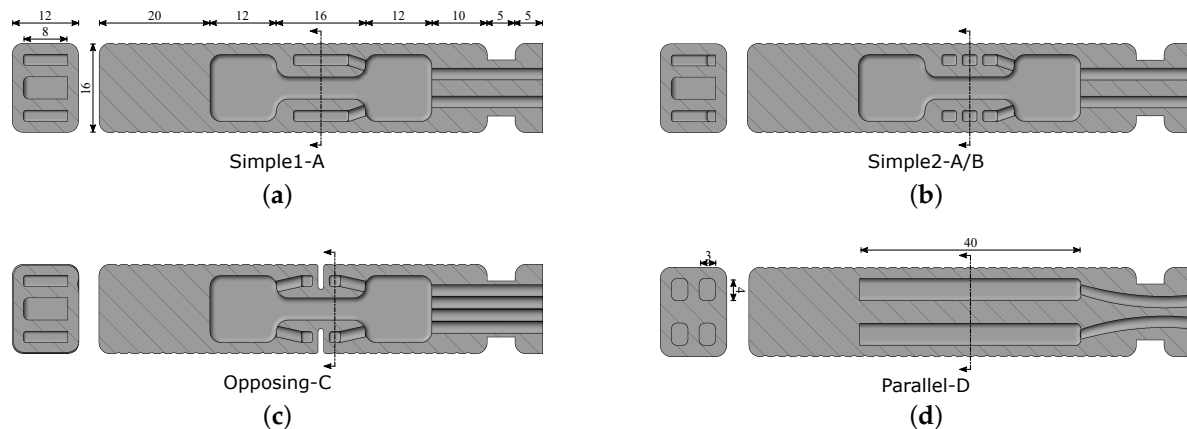


**Figure 1.** Transverse (left) and longitudinal (right) cross-sections of the four internal geometries used in the fabricated prototypes, showing insertion routes for the input tubing. (a) Simple1, simple side-pockets without supporting internal walls; (b) Simple2, simple side-pockets with two supporting internal walls; (c) Opposing, opposing side-pockets; (d) Parallel, four parallel pockets.

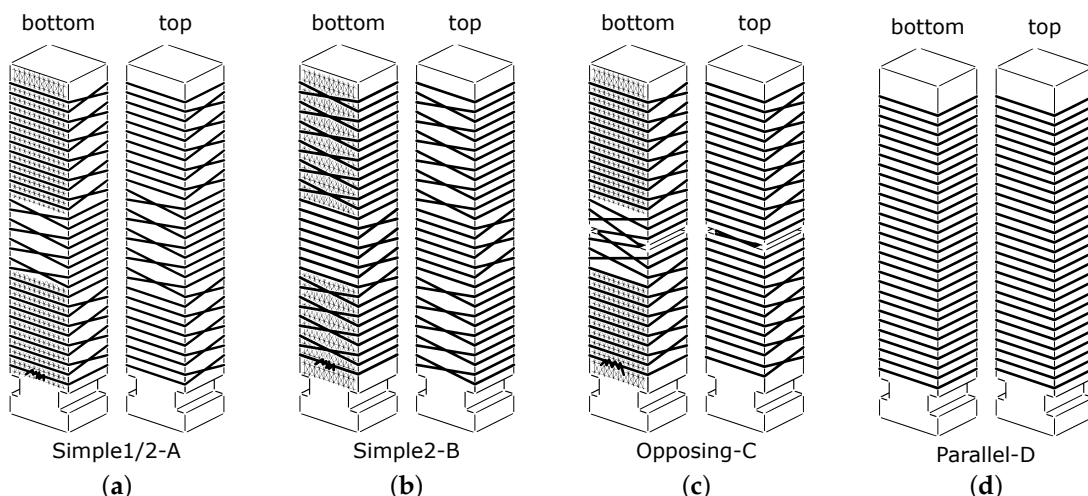


**Figure 2.** The four different reinforcement layouts used in the fabricated prototypes. (a) A, two-directional thread winding, crossing itself on the bottom and top in the middle and on the sides otherwise; (b) B, two-directional winding, crossing in the opposite manner from A; (c) C, two-directional winding, crossing itself mainly on the bottom and once on the top in the middle; (d) D, single loops. A, B, and C had a strain-limiting layer under them, excluded from middle, while D had only the radial reinforcement thread.

#### 2.4. Simple Side-Pockets

The first design, Simple1, had simple side-pockets for abduction-adduction on the sides of a bigger central pocket for flexion (Figure 1a). For this design, we made a variation, Simple2, which had supporting internal walls in the abduction-adduction pockets (Figure 1b). The goal was to test whether the supports would affect the actuators' response. Without supporting walls, the pockets were expected to balloon freely, leading to a relatively large sideways expansion, including towards the inside of the

actuator. This expansion was expected to be limited by the supporting walls, thus directing it more towards the actuator's tip and increasing the force output in the wanted direction.

The reinforcement helix was wound around the prototypes from the root to the tip and back again. Thus, it crossed itself twice every round. Prototypes Simple1-A and Simple2-A had the helix crossing itself on top and bottom of the actuator in the center 16-mm part (Figure 2a). This way, the thread was aligned straight and evenly on the sides. On the other parts of the actuators, the helix crossed itself on the sides. For prototype Simple2-B, the helix was wound in the opposite fashion (Figure 2b).

A strain-limiting layer made of rayon net was embedded inside the silicone wall under the actuators (Figure 2a,b). The middle region was left free to let the actuators expand in length around the curvature of the MCP joint and to reduce the effect of flexion structures on the abduction-adduction function.

## 2.5. Opposing Side-Pockets

The second design (Figure 1c) had two opposing pockets on each side of the flexion pocket. This design of the side-pockets, sometimes referred to as *bellows-type* [30] or *pleated type* [31], relied on opposing ballooning structures that press against each other to cause a bending motion. The side-pockets had their thinnest wall (1 mm) on the side on which the deformation needed to be largest, i.e., where the two walls were to press against each other.

We considered the main advantages of the opposing pocket structure to be that it would concentrate the deformation to a limited area, leading to a more pivot-like response for abduction-adduction, and separate it from the flexion function.

For the prototype Opposing-C, the reinforcement helix was wound so that it was always crossing itself on the sides, except in the center, where it crossed itself under the actuator, and once on top, as it passed through the gaps between the opposing pockets (Figure 2c). The strain-limiting layer was embedded under the actuator in the same way as with the Simple prototypes, leaving the abduction-adduction part of the bottom free.

## 2.6. Parallel Pockets

The third prototype design (Figure 1d) was based on the idea of using multiple long pockets laid out in a symmetrical pattern along the length of the actuator. Differential inflation of the pockets would provide more control over the deformation, so that the finger joint motions could be adjusted to match the target motions.

With a three-pocket design, it would be possible to achieve a full 360° directional control of an actuator's free bending, as shown by Gerboni et al. [15]. However, in the case of hand motion assist, the major difference is that the finger presents an extra constraint for the actuator. Furthermore, the MCP joint has two perpendicular DoFs that we want to control separately. These aspects add specific restrictions for actuator geometry, which need to be considered in order to achieve and control the wanted motions.

Using a four-pocket design, with pockets in a square pattern (Figure 1d), it would be possible to control the flexion-extension and abduction-adduction motions by applying pressure to two pockets at a time and adjusting their relative pressures. For example, actuating the top pockets would make the top of the actuator expand, while the passive, relatively thicker bottom layer would limit the expansion, which would lead to a flexion motion. Similarly, when one or two left side pockets are inflated, the actuator would bend to the right, leading to abduction-adduction motion.

The prototype Parallel-D had only the reinforcement fibers around it, in single loops for symmetry (Figure 2d), to restrict the radial expansion. We did not include a strain-limiting layer, as the actuator's operating principle was based on structural symmetry and differences in relative silicone thickness on the actuated and non-actuated sides.

### 3. Prototype Fabrication and Evaluation

The function of the described actuator designs was validated by fabricating and testing the five prototypes. In this section, we will describe the fabrication methods for making the prototypes and the evaluation methods (trajectory and torque measurements) for testing and comparing them.

#### 3.1. Fabrication

The actuators were fabricated out of a two-part platinum curing silicone, Dragon Skin 10 Slow, by using 3D-printed molds and embedded reinforcing materials. Silicone glue, Sil-Poxy, was used for input tubing attachment, fixing possible delaminations, etc. Rayon net with approximately a  $1\text{ mm} \times 2\text{ mm}$  mesh was used for the strain limiting layer, and 0.7 mm-thick cotton string was used for the reinforcement fiber. Silicone tubing was used for connections in the actuators and for connecting to the pressure sources. The molds were printed out of Polylactic Acid (PLA).

We used two different casting workflows for making the tested prototypes' main body, i.e., the pocket structure. The first was used for the prototypes with simple side-pockets and opposing pockets and the other for the parallel pocket prototype.

The first workflow had two molds. The first mold was used for casting the top part of the silicone pockets. Insertion holes for the input tubing were created by attaching 2 mm diameter steel sticks to the mold. After casting the top of the actuator structure, the input tubing was placed into the holes and glued in place with silicone glue. The second mold was then used for closing the pockets. In this step, the strain limiting layer was laid out in the mold so that it got embedded inside the 2 mm-thick enclosure. The rayon net was laid out in three layers, which were aligned in a  $45^\circ$  angle relative to each other. This arrangement made the composite layer become practically inextensible and strong against delaminating forces, but still highly flexible.

The parallel pocket prototype had only one mold. Furthermore, input tubing was placed in the mold before casting, which reduced the required work. The tip parts of the pockets were open after casting the main body and were closed by gluing a silicone glue-filled 2 cm-long silicone tube into them.

The last step in making the prototypes was the winding of the reinforcement helix around them by hand. The cotton string was fixed in place by pouring a layer of silicone on it. The silicone was allowed to cure by hanging the actuators freely tip down from the input tubing. This ensured an even distribution of silicone on all sides, reducing response changes caused by uneven wall thickness. The final prototypes are shown in Figure 3.

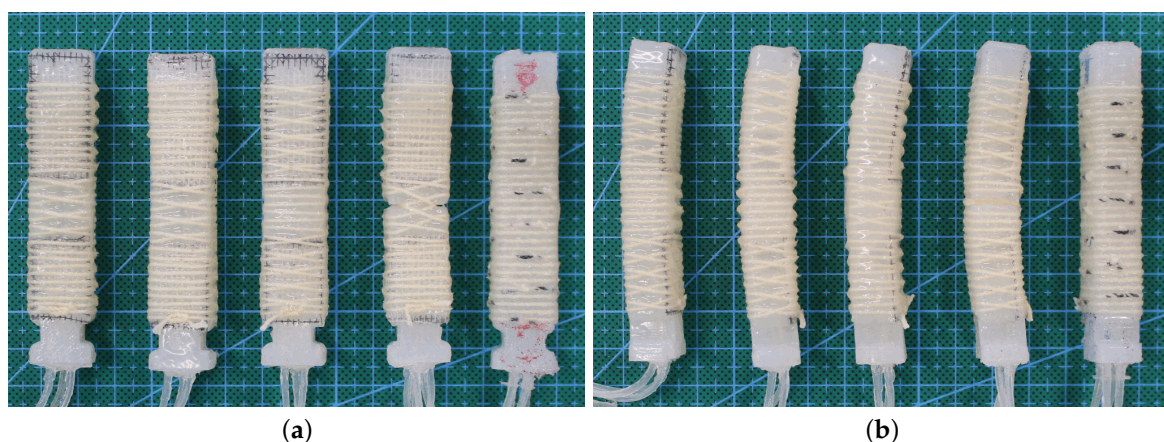


**Figure 3.** The five prototypes shown from the (a) bottom and (b) right. From left to right: Simple1-A, Simple2-A, Simple2-B, Opposing-C, Parallel-D.

We produced the single loops for D-type reinforcement (Figure 2d) by opening the windings of a single thread into three separate strands, and winding each one twice around itself on the actuator.

Thus, we got three separate three-strand loops. The ends of the strands were locked in place with a reef knot.

### 3.2. Trajectory Measurements

The goal of the free trajectory measurements was to evaluate the designed prototypes' RoM, possible deviations from the wanted straight trajectories and the symmetry of their motions. This gave us information on how well the designed structures could generate motion without having their two functions affect each other.

The prototypes' 3D-trajectory was measured with a three-camera motion capture system, attaching a marker cluster, shown in Figure 4, on the actuator tip. The measurements were done at 0–225 kPa pressures, with 50-kPa intervals. However, the opposing pocket prototype had a maximum pressure of 175 kPa for abduction-adduction, because of its pockets' large deformation. For measurements with two pockets inflated at the same time, the pressure was input from the same source to both pockets, so that their pressure was equal.

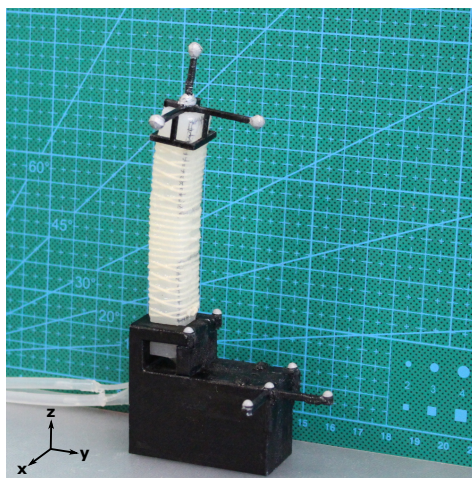


**Figure 4.** Motion capture marker setup for trajectory measurements. The two center markers on the tip of the actuator formed its tip vector. Other markers were used as a reference.

As the parallel pocket prototype was symmetrical, the trajectory measurements for flexion were done twice. From here on, we refer to these two measurements as top up and bottom up.

### 3.3. Torque Measurements

The goal of the torque measurements was to evaluate how well the actuators could transfer their deformation to forces in the wanted directions and thus apply the required torques on a human finger. As with the trajectory, we were especially interested in the prototypes' output torque range and its symmetry.

For practical and safety reasons, the torque measurements were done by coupling the actuators to a two-bone dummy finger (Figure 5), which was scaled to match the dimensions of a middle finger [29]. The 3D models used were acquired from Thingiverse (Human Hand Bones-Thumb by siderits and Ball-Socket Joint by BrainSTEM) [32]. The combined finger structure was 3D-printed and attached to a clamp that held the prototype in place. A steel wire connected to a force gauge was attached to the tip of the distal bone.

The length of the dummy finger's proximal phalanx, from the joint center to the attachment point, was  $r = 49$  mm. The force gauge was always kept in a right angle to the bone, and the joint angle was changed by tilting the clamp. Thus, the torque at the joint was:

$$\tau = rF. \quad (1)$$

The dummy joint was set to specific angles:  $0^\circ$ ,  $30^\circ$  and  $60^\circ$  for the flexion measurements and  $0^\circ$  and  $20^\circ$  for abduction-adduction. The finger was restrained from flexing in the abduction-adduction measurement with a fixed PTFE (Polytetrafluoroethylene) block. This ensured that the wire stayed always at a right angle.

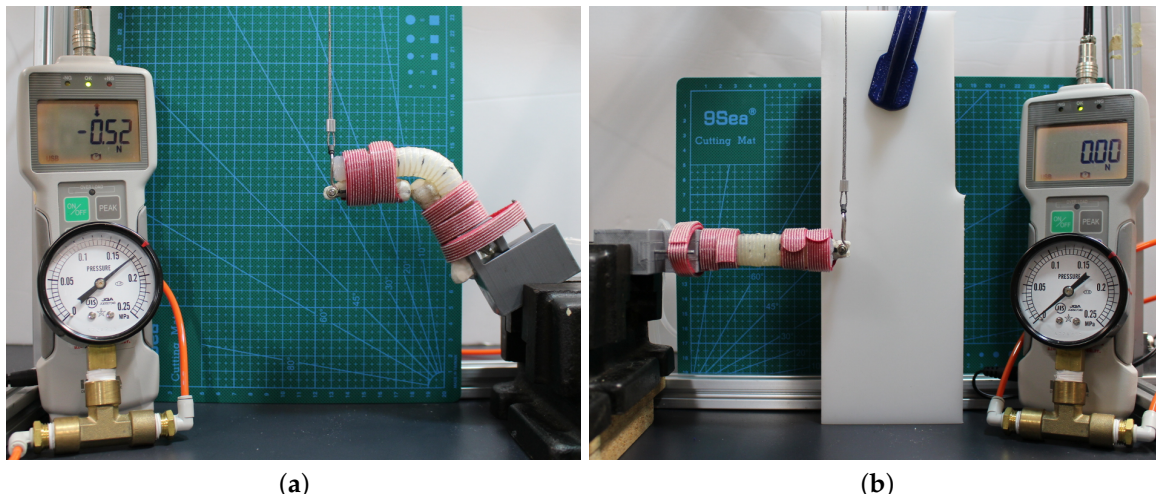


**Figure 5.** Torque measurement setup with the dummy MCP joint. The joint angle was set to  $0^\circ$ ,  $30^\circ$  and  $60^\circ$  for flexion and  $0^\circ$  and  $20^\circ$  for abduction-adduction, keeping the distal bone perpendicular to the force gauge (above). Joint torque was then calculated from the measured force. (a) Parallel-D flexion,  $60^\circ$ , 175 kPa; (b) Parallel-D abduction-adduction to the right,  $0^\circ$ , 0 kPa.

The forces were measured at a 0–225 kPa pressure range, with 25-kPa intervals. The maximum pressures for each prototype were defined by observing the actuator's deformation, keeping the pockets from expanding too much in order to minimize plastic deformation. The minimum pressure for the angled measurements was different for each prototype. It was defined as the pressure at which the actuators reached the target angle. Simultaneous inflation of two pockets, for opposing and parallel pocket prototypes, was done by connecting both to the same pressure source, as in the trajectory measurements.

Each flexion measurement was repeated 10 times, and each abduction-adduction measurement 15 times, for each pressure. As with the trajectory measurements, the parallel pocket prototype was measured twice in the flexion direction to determine the symmetry of its torque output. The prototype was turned around, and the opposite side pockets were inflated. As before, top up and bottom up are used to distinguish the two measurements.

#### 4. Results

In this section, we present the results of the trajectory and torque measurements. The full set of numerical data and more photos of the experiments are available as supplementary materials.

##### 4.1. Trajectory, Flexion

The flexion trajectory measurement results are presented in Table 1 and Figure 6.

**Table 1.** Maximum actuator tip angles for flexion trajectory measurements.

	Simple1-A	Simple2-A	Simple2-B	Opposing-C	Parallel-D Top Up/Bottom Up
Flexion RoM	$160^\circ$	$184^\circ$	$166^\circ$	$208^\circ$	$107^\circ$ / $103^\circ$

Looking at Table 1, we can see that all designs fulfilled the required RoM, bending past  $100^\circ$ . Opposing-C had the largest flexion RoM of all of the prototypes, while Parallel-D had the smallest. Of the simple side-pocket prototypes, Simple2-A was flexing slightly more (approximately  $20^\circ$ ) than the others. Notably, the difference between these prototypes was the internal structure for Simple1-A and the reinforcement helix layout for Simple2-B.

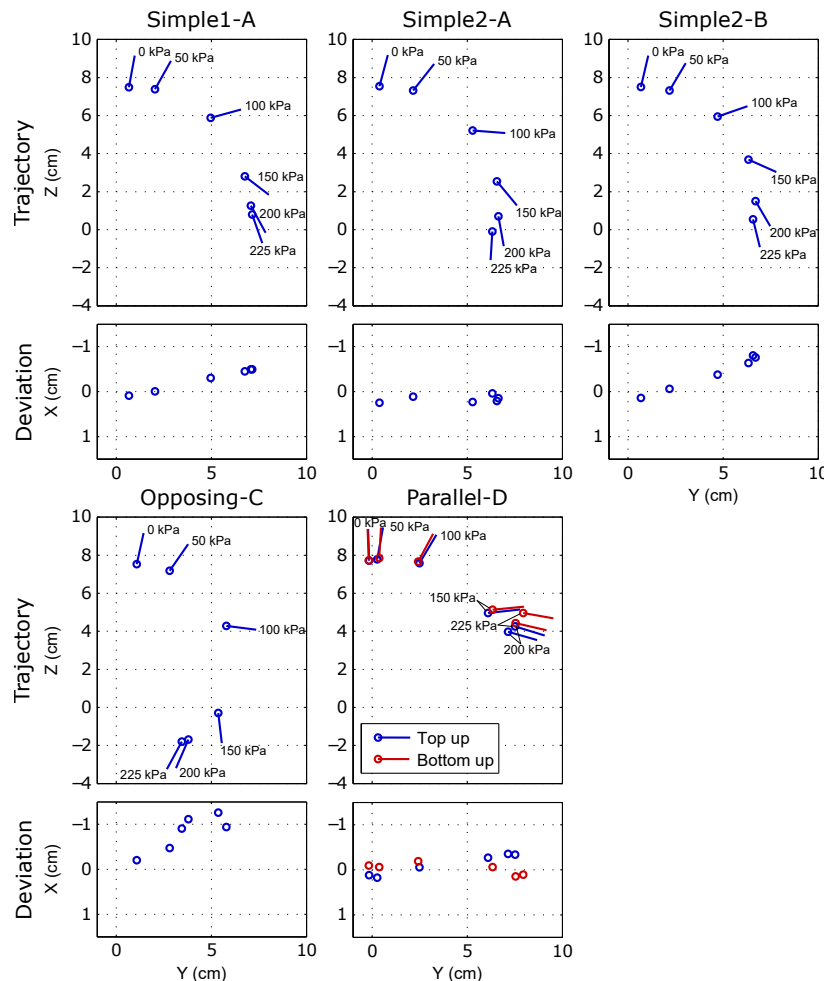


**Figure 6.** Flexion trajectory results, showing the motion of the actuator tip vector formed by two markers. Only the Simple2-A and Parallel-D prototypes stayed in a relatively straight trajectory. The others tended to turn to the left. Lengthwise extension is visible as the tip marker's deviation from a round trajectory. For Parallel-D, it is possible to see an end of the flexion motion, after which only lengthwise extension occurred.

Of all the prototypes, Simple2-A and Parallel-D had the straightest flexion trajectories, while the others showed more deviation from the centerline (Figure 6). This deviation was strongest for Simple2-B and Opposing-C, which deviated approximately 1 cm to the left from their starting point.

All of the actuators had a similar nonlinear pattern in their bending (Figure 6). The first 50 kPa of pressure had only a small effect, but a large deformation happened between 50 kPa and 200 kPa. The actuators also had a limit to their bending at approximately 200 kPa. After this, they mainly continued to extend in the lengthwise direction, instead of increasing the flexion angle further. This can be seen most clearly for prototype Parallel-D, which has the tip vector making a big jump between 100 kPa and 150 kPa and then moving away from the center ( $z$ -axis), instead of going down, between 200 kPa and 225 kPa. The lengthwise extension can be seen also for the other prototypes as a deviation from a round trajectory. This deviation was smallest for Opposing-C.

#### 4.2. Trajectory, Abduction-Adduction

The results of abduction-adduction trajectory measurements are presented in Table 2 and Figure 7.

**Table 2.** Maximum actuator tip angles for abduction-adduction trajectory measurements.

	Simple1-A	Simple2-A	Simple2-B	Opposing-C	Parallel-D
Abd-Add RoM to left	42°	40°	30°	54°	139°
Abd-Add RoM to right	39°	40°	30°	38°	135°

All of the prototypes passed the required limit of 20° angle in both directions with at least a 10° margin (Table 2). For prototype Opposing-C, there was a notable (16°) difference between abduction-adduction RoM to the left and right. However, based on our observations, this asymmetry was mainly caused by stronger ballooning of the opposing pockets on the right side of the prototype. For the other prototypes, the difference was relatively small.

On the other hand, all of the prototypes had a deviation from the desired straight trajectory (Figure 7). This was most pronounced for Simple1-A. Comparison between the simple side-pocket prototypes shows that Simple2-B (Figure 7) had asymmetry between the deviations to the left and right, with the motion to the left being straight. For Simple1-A and Simple2-A, the deviation was fairly symmetrical. Furthermore, for Simple2-A and Simple2-B (to the right), the deviation was approximately half of that of Simple1-A. Furthermore, Parallel-D showed deviation from a straight trajectory regardless of its symmetrical design. The actuator was flexing slightly in front during motion to the left and slightly to the back during motion to the right.

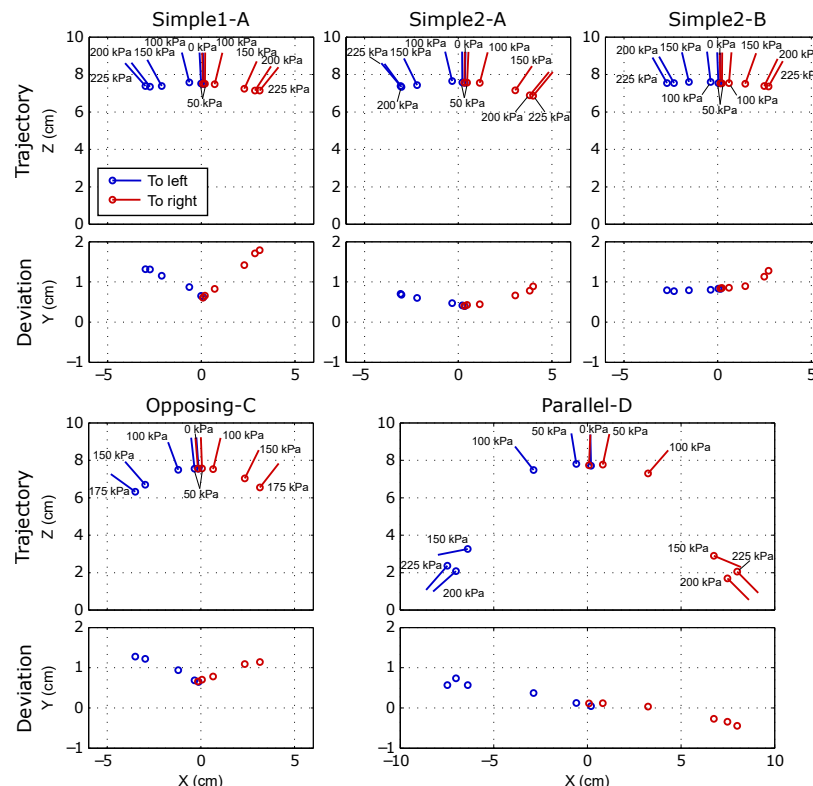


**Figure 7.** Abduction-adduction trajectory results. Lengthwise extension can be seen as straight motion of the tip to the sides, instead of a round curve. Opposing-C had the roundest motion and least lengthwise extension, and it behaved most like a pivot joint. Parallel-D had a wider motion than the others due to its different structure and had the largest lengthwise extension. It is also possible to see the actuators' nonlinear motion pattern, similar to the flexion measurements.

The nonlinear bending phases and lengthwise extension are visible also in the abduction-adduction results for all prototypes (Figure 7), in the same manner as in flexion. The effect was again especially pronounced for Parallel-D.

#### 4.3. Torque, Flexion

The results of flexion torque measurements are presented in Table 3 and Figure 8.

**Table 3.** Maximum average joint torques for flexion.

	Simple1-A	Simple2-A	Simple2-B	Opposing-C	Parallel-D Top Up/Bottom Up
Flexion 0°	17.68	18.04	17.12	16.10	15.03/15.43 (Ncm)
Flexion 30°	11.23	10.13	14.34	16.57	10.04/11.26 (Ncm)
Flexion 60°	5.23	6.06	7.22	7.64	9.42/9.75 (Ncm)

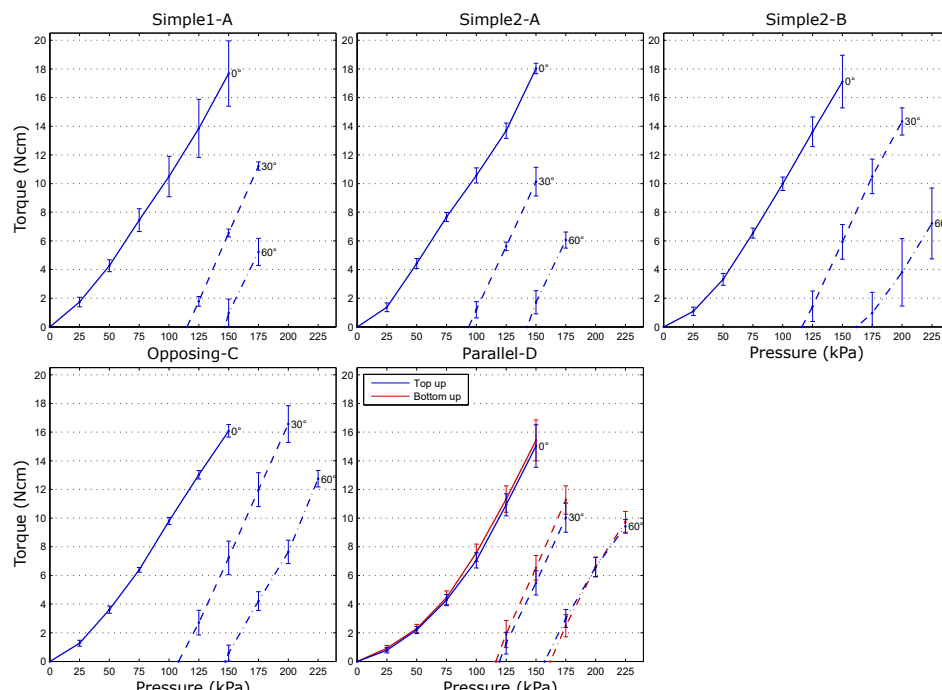


**Figure 8.** Torque measurement results for flexion at 0°, 30° and 60° flexion angles, with sample standard deviations. The maximum pressures for Simple1-A and Simple2-A were limited to avoid ballooning of silicone between the reinforcement helix on the back of the actuators.

The results in Figure 8 and Table 3 show that all actuators decreased their maximum torque output with higher angles of flexion. This effect was strongest for Simple1-A and Simple2-A, which both had an approximately 12-Ncm (70%) drop between 0° and 60°, while for Opposing-C, this drop was approximately 3.4 Ncm (21%) and for Parallel-D 5.6 Ncm (40%).

Simple1-A and Simple2-A had their maximum flexion pressure limited to 175 kPa, because the silicone started to bulge between the reinforcement windings on top of the actuators. Thus, we restricted the maximum pressure, to prevent plastic deformation. On the other hand, Simple2-B had the winding in the exact opposite order, which allowed the maximum pressure to be higher, as ballooning did not happen. Furthermore, Opposing-C had a more uniformly-distributed winding on its top and could reach higher pressures. For Parallel-D, the limitation for each measured angle came from it starting to direct its deformation into unwanted directions at higher pressures, as the prototype could not move the joint further into flexion.

Notably, the torque outputs and applied pressures for Simple1-A and Simple2-A were similar at  $0^\circ$ , but at higher flexion angles, especially at  $30^\circ$ , Simple1-A required higher pressures to reach the same torque outputs. On the other hand, Simple2-B had a slightly lower torque output than Simple1-A and Simple2-A and required higher pressures for higher angles.

Figure 8 shows that there was only a small difference between Parallel-D's top up and bottom up measurements. The actuator seemed to have a slightly lower torque output when it was placed top up, except for the  $60^\circ$  joint angle. However, this difference was mostly within the deviations.

#### 4.4. Torque, Abduction-Adduction

The torque measurement results for abduction-adduction are presented in Table 4 and Figure 9.

**Table 4.** Maximum average joint torques for abduction-adduction.

	Simple1-A Left/Right	Simple2-A Left/Right	Simple2-B Left/Right	Opposing-C Left/Right	Parallel-D Left/Right	
Abd-Add $0^\circ$	4.08/4.79	3.87/4.79	3.11/4.14	4.46/3.64	9.10/9.23	(Ncm)
Abd-Add $20^\circ$	3.13/2.89	3.09/3.30	1.85/2.07	2.58/2.01	5.90/5.91	(Ncm)

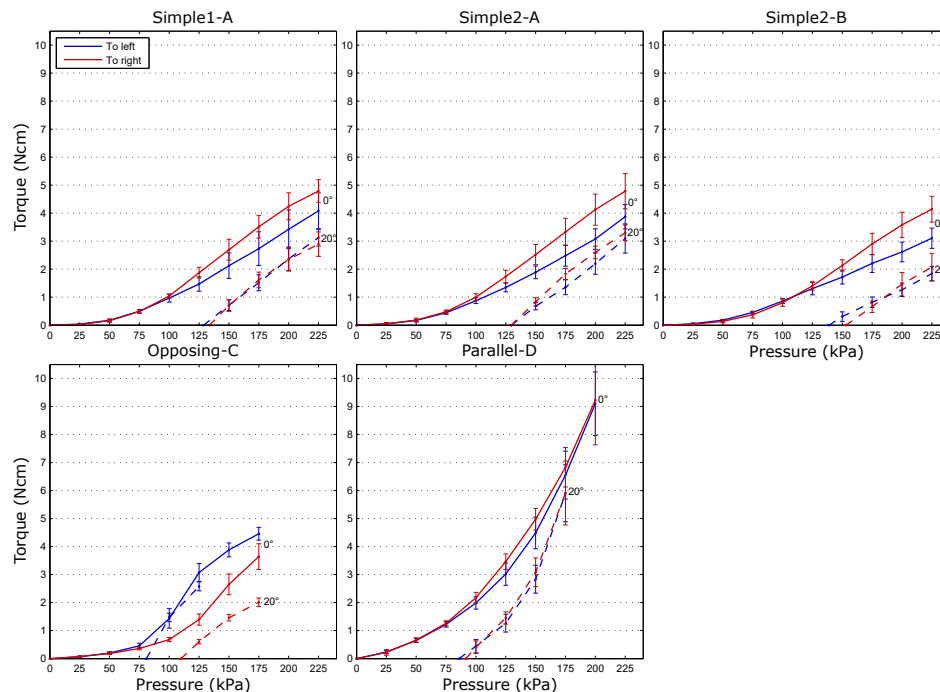


**Figure 9.** Torque measurement results for abduction-adduction at  $0^\circ$  and  $20^\circ$  angles, with sample standard deviations. Maximum pressure for Opposing-C was limited to reduce the ballooning of the pockets and in the end, because of the right side pockets' excessive ballooning. For Parallel-D, the limitation was due to the actuator starting to twist in unwanted directions, which can be seen also as a notable increase in the standard deviation.

Differences between the simple side-pocket prototypes appeared also in the abduction-adduction measurements. Furthermore, they all showed a tendency of pushing harder to the right. Simple2-B had the weakest response comparing to Simple1-A and Simple2-A, with the average maximum abduction-adduction torque being 3.5 Ncm, while for the others, it was slightly above 4.0 Ncm.

Opposing-C had a notable difference in its motions to left and right. Based on our observations, this was caused by the opposing pockets ballooning differently on each side. However, its torque

range was similar to Simple2-B, while the difference to the other simple side-pocket prototypes was not big either.

Parallel-D had the highest and most symmetrical torque output in the abduction-adduction test. This was expected, as its structure for this function was basically the same as for flexion, while the other prototypes had a specialized structure for abduction-adduction.

Figure 10 shows the prototypes' deformation during the 20° abduction-adduction measurements. Comparison between the photos showed that prototypes Simple2-A and Simple2-B had approximately a 13% and 6% smaller inflated width than Simple1-A, respectively. Figure 10e,j shows how Parallel-D pushed to the side, away from the joint center, because of its excessive lengthwise extension.

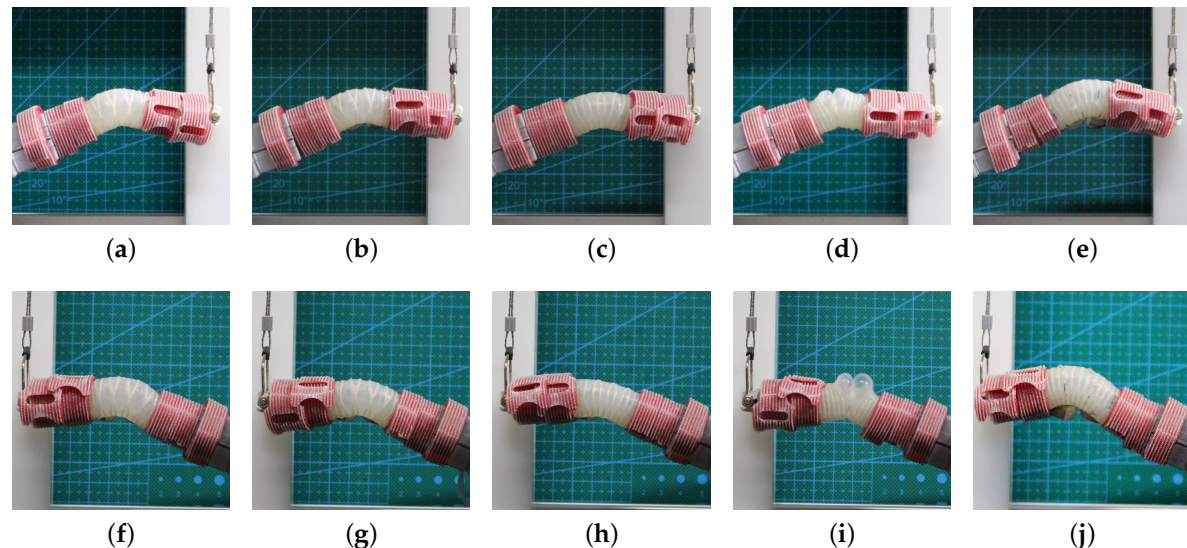


**Figure 10.** Prototype maximum deformation in 20° abduction-adduction torque measurement to the right (a–e) and to the left (f–j); (a,f) Simple1-A, 225 kPa; (b,g) Simple2-A, 225 kPa; (c,h) Simple2-B, 225 kPa; (d,i) Opposing-C, 175 kPa/125 kPa. Photos were taken at the end of the measurements, when the right side pockets' ballooning had become excessive; (e,j) Parallel-D, 175 kPa.

## 5. Discussion

In this section, we discuss the potential of our three functional design approaches (Simple, Opposing and Parallel) to making a multi-pocket actuator for 2-DoF MCP joint motion assist. First, we consider and explain the differences between the five prototypes' response and compare them to related studies. Then, we discuss how the actuator structures could be improved to meet the requirements. Finally, we will state our plans for future work.

### 5.1. Comparison of Prototype Performance

We observed distinct differences between our prototypes' response, which can be connected to their geometry and reinforcements. Each of them had clear advantages and disadvantages comparing to the others. A comparison of the prototypes is summarized in Table 5.

#### 5.1.1. Coupling between Actuator Functions

Our main goal was to evaluate the separation of the control of the MCP joint's two DoFs. In other words, we wanted to see how each prototype's passive inputs and their functional structures affected the active inputs that were designed to move a single DoF.

In Table 5, we give our qualitative approximation of the prototypes' relative ability with regard to this. For the relative ranking, we considered several aspects of the prototypes' response. These were the actuators' deviations from the wanted straight trajectories, the relative strength of torque output

between flexion and abduction-adduction and the approximate amount of different functional structures that clearly affected another function negatively.

**Table 5.** Comparison of tested prototypes; advantages and disadvantages of each approach and relative level of coupling between the two functions.

Prototype	Advantages	Disadvantages	Coupling between Functions
Simple1-A	N/A	Gaps in reinforcements cause ballooning; wide radial expansion	High
Simple2-A	Strong structure; limited radial expansion	Gaps in reinforcements cause ballooning	Medium
Simple2-B	N/A	Reinforcement alignment weakens output and causes deviation to left in flexion	High
Opposing-C	Pivot-like sideways response; strong flexion	Excessive ballooning of side-pockets; sideways flexibility; asymmetric response	High
Parallel-D	360° control; potential to adapt to thumb support	Excessive length extension	Low

Of the three simple side-pocket prototypes, Simple2-A seemed to be slightly better than the others with regard to separating the two functions. They all had varying degrees of deviation from a straight trajectory. For flexion, Simple2-B had the largest deviation, while Simple1-A had some, and Simple2-A had none. For abduction-adduction, the most affected prototype was Simple1-A with relatively asymmetric and strong deviation to the front in both directions. The other two had the internal supporting structures restricting this deviation. The supports also proved to be efficient in making Simple2-A's response stable, limiting its radial expansion (Figure 10) and its deviation from the wanted trajectory in abduction-adduction (Figure 7), compared to Simple1-A. Interestingly, Simple2-B had a relatively straight trajectory to the left in abduction-adduction, but not to the right. The only reason for this we can think of is the asymmetry of the reinforcement thread. For torque, the limitations of the A-type reinforcement helix were apparent, as input pressures had to be limited (Figure 8) due to silicone ballooning on the back of the two actuators. However, although Simple2-B could reach higher pressures and flex more, its reinforcement helix made its response unstable. It had a relatively large standard deviation in the measurements and was bending to left in flexion (Figure 6). Furthermore, the central part of these actuators was extending only in length, as it had no flexion-enhancing strain-limiting layer.

Opposing-C's opposing pocket structure showed its potential in providing large, localized displacements in abduction-adduction (round trajectory in Figure 7), and its motion seemed most like that of a hinge joint (Figure 10). In other words, the center of rotation changed only slightly and stayed approximately above the joint. The other prototypes had a clear curvature and change in their center of rotation. Opposing-C also had the highest flexion tip angle (Table 1). However, the strong flexion was caused by the bottom side's reinforcement helix in the central part (Figure 2c). It restricted expansion on that side and caused flexion during abduction-adduction. Furthermore, its asymmetry caused the flexion to deviate strongly to the left (Figure 6). These effects were amplified by the gaps between the opposing pockets, which made the central part of the actuator much more flexible and unstable than the other prototypes.

Parallel-D's symmetrical design had a clear advantage over the other approaches. It allowed the actuator to bend and provide torque in both flexion and abduction-adduction directions in an equal way. The differences were mainly caused by the rectangular shape of the actuator and the connection

to the dummy joint, which caused the difference in RoM and the lower torque in abduction-adduction, respectively. The prototype's free flexion RoM was also limited as it did not have a structure to restrict its lengthwise expansion. However, when connected to the joint, its expansion was directed by constraints from the connecting straps and the dummy joint's rigid structure. The prototype had some deviation from straight trajectories for both flexion and abduction-adduction (Figures 6 and 7). However, this deviation seemed to be symmetrical. Thus, it may have been caused by small symmetrical inaccuracies in fabrication and was probably not related to the design approach itself. Possible unequal pressure in the pockets can be ruled out, as the input was the same for both.

In summary, all three design approaches were promising in providing 2-DoF support for the MCP joint. However, all of the prototypes had some issues with the connection between the functions. These need to be solved in order to make the actuators plausible for use in power-assist for rehabilitation.

### 5.1.2. Range of Motion and Torque

All of the prototypes met the set flexion RoM requirements (Table 1). This seems to be normal for this type of actuator [12,14,16–18,20], as they tend to enable large displacements easily. This shows also that our multi-pocket designs did not degrade the flexion function in a notable way. Furthermore, the bending angle relative to input pressure could be adjusted further by, e.g., changing the pockets' length. This can be seen from our previous results [18] and the data of Polygerinos et al. [20].

Furthermore, the abduction-adduction RoM requirements were met (Table 2). However, a comparison with other similar soft actuators for hand rehabilitation is not possible, as the motion has not been studied before. Still, making an analogy with Ueki et al.'s rigid hand rehabilitation mechanism [33] is possible. It could reach a 30° abduction-adduction angle, when connected to a patient's index finger. Furthermore, considering only Parallel-D's response, Gerboni et al. got comparable results for their three-pocket soft actuator module [15]. They reached a free bending angle of approximately 75° by inflating one pocket, although with much lower pressures (up to 35 kPa), as their actuator was 25 mm long, its diameter only 9 mm and its walls much thinner. On the other hand, a previous, 35 mm diameter version of their actuator reached a free bending angle of 120° with one pocket and 80° with two, at 65 kPa [34].

The prototypes also provided torque to the joint in both flexion and abduction-adduction, throughout the measured joint angle range. However, none of them reached the set torque specifications. We connected the prototypes to a dummy finger in order to measure their practical output torques easily and safely. This allowed us to disregard the effects of soft tissues and the possibility of a test subject assisting or resisting the actuator's motion. However, it is difficult to find comparable results from previous soft actuator studies, as this type of measurement has not been used commonly. Furthermore, none of the previous studies have considered abduction-adduction.

Still, an approximate reference for flexion can be found from a study by Noritsugu et al. [12]. Their actuator's MCP joint supporting force was 14 N at the "root of the finger", while wearing the glove. Assuming that the measurement point was the center of the index finger proximal phalanx (palmar digital crease), the moment arm would have been approximately 2 cm [29]. Thus, their actuator's flexion torque on the MCP joint would have been approximately 28 Ncm, which would make their actuators somewhat stronger than ours (Table 3).

Previous studies have often measured the actuators' tip force output by clamping them from one end into a horizontal position, and restricting vertical deformation with a solid structure directly above them, as well as a force sensor set under the tip [14,18,20]. For calculating the torque, we assume that the lever arm was half of the length between the two end supports. Our previous flexion prototypes could reach a 10 N maximum force with a 3.25 cm lever arm at 150 kPa, i.e., a torque of 32.5 Ncm [18]. On the other hand, Polygerinos et al. reached an 8 N force with a 13 cm-long fiber-reinforced actuator at 200 kPa, i.e., 52 Ncm [20]. Finally, Yap et al. reached 14 N with their 15–18 cm-long fabric-based

actuators at only 70 kPa, i.e., 105–126 Ncm [14]. Although these torques cannot be directly compared to our results, they give some reference to how our prototypes performed.

A further, more valid comparison can be made with the rigid mechanism by Ueki et al. [33]. Their device could reach a maximum MCP joint torque of 51 Ncm for flexion and 79 Ncm for abduction-adduction, which were both several times higher than for any of our prototypes.

All prototypes decreased their maximum torque output at higher bending angles (Figures 8 and 9, Tables 3 and 4). This appeared to be highly dependent on the actuator design and the maximum pressures they could reach. However, the behavior seems to be normal for this type of soft actuator, which can be confirmed from previous results obtained by Noritsugu et al. [12]. Their measurements showed a torque drop of approximately 60%, between 0° and 60° angles at constant 320 kPa, for their curling soft actuator for elbow flexion. On the one hand, minimizing the rate of this change would be beneficial, considering control system design, as the response would be more predictable. On the other hand, this could be seen as an advantage of using soft actuators, regarding safety, as they naturally reduce the applied forces, when bending the joint further.

### 5.1.3. Safety and Reliability

Safety and reliability must also be taken into consideration, when designing assistive technologies. One of the main dangers of soft fluidic actuators is related to material failure, leading to rupture and a sudden release of pressure [5]. Thus, ideally, the actuating pressures should be as low as possible, while providing adequate forces for assisting the joint motions.

For Simple1-A, Simple2-A and Opposing-C, the large deformation of the material between the reinforced parts exposed the actuators to plastic changes, which is evident especially in Figure 10i. The results showed this clearly, as the simple side-pocket prototypes' maximum flexion pressures were limited, and for Opposing-C, the final torque measurements to left and right were completely different (Figure 9). This ballooning of the silicone made the prototypes vulnerable as they got exposed to the environment. Considering these aspects, prototype Parallel-D's single loop reinforcement was the most effective in keeping the response unchanged and preventing the silicone from bulging from between the thread.

Another danger is that the actuators might apply twisting or longitudinally pulling forces to the assisted fingers. In excessive amounts, such forces could cause dislocations of the joints. These forces were not measured in the current study, but based on the trajectory data in Figures 6 and 7 and our observations during the torque measurements, the tested prototypes did not have a tendency to twist or pull excessively. The only exception was Parallel-D's strong lengthwise expansion. In the current experiments, this was not a problem as the torques were relatively low (Figures 8 and 9, Tables 3 and 4). However, this would be good to take into consideration in the future, when evaluating safety.

## 5.2. Actuator Structure Improvements

In this section, we discuss possible improvements for our actuator designs. First, we consider some general improvements that could be applied to all of them, and then, we concentrate on the disadvantages of each approach separately.

The lack of torque output can be overcome by improving key parameters of the structure. For example, making walls thicker would affect the stiffness of the actuator body, meaning higher pressures and stronger output. The scaling of actuator geometry has been considered before by e.g., Deimel and Brock [16], who calculated a scaling law for this type of actuator. They concluded that actuator stiffness scales to the fourth power of its size, which can be used effectively for adjusting their strength. However, a balance should be found between strong output and safety.

The nonlinearly changing pattern of the prototypes' motion relative to the input pressure was due to them first expanding from rectangular into a rounder cross-section and only then starting to bend, as this radial expansion got limited. This could be improved by making their pockets and cross-section rounder, which would reduce the required initial expansion of the structure before the

point when the actual motion starts. It would also lower the required pressure, making the actuators safer [5]. For example, Polygerinos et al. have considered the effects of changing the shape of the actuator body [20]. This improvement, however, is limited by the placement of the actuator on top of a finger and the connection between the two. Furthermore, the relative placement of the multiple pockets in the actuator structure needs to be considered.

The asymmetric reinforcement helix was the main reason for simple side-pocket and opposing pocket actuators' deviation from the wanted motions. The parallel pocket prototype's single loop reinforcements did not seem to cause a similar effect. In fact, the two-directional winding, with its angled thread, is not necessary for achieving our target functions, as twisting of the actuator around its axis is not included in the wanted motions. It has mainly been used, throughout the field, due to ease of fabrication, as a single thread can be quickly wound around the actuator body to provide restriction to radial expansion. Thus, to work around the problem of asymmetric response, the reinforcement would be best made as single loops, as we did with Parallel-D. This would also help with distributing the reinforcement homogeneously and at high enough intervals, to make sure there is no excessive local ballooning of the silicone between gaps in the reinforcement. However, the fabrication methods need to be improved, as our current method for producing the single loops is very time consuming and tedious.

### 5.2.1. Simple Side-Pockets

Simple2-A showed the most potential of the three simple side-pocket prototypes. However, the imbalance of its abduction-adduction response and the conflict between its two functions would need to be solved to make it plausible for use in power-assist. The lack of a flexion-inducing strain-limiting layer in the central part of the actuators is problematic. It is a compromise of weakening flexion to reduce the two functions' effect on each other. Thus, a way of strengthening the flexion without affecting abduction-adduction should be found in order to counter this problem.

One idea is an active control of the strain-limiting structures, or in other words, a stiffness-controllable structure. An example of this is the negative pressure jamming structures in a study by Wall et al. [35]. Basically, by changing the state of this structure, we could choose between flexion and abduction-adduction. However, this would add more inputs to control and should be considered carefully.

Another possible way of solving the problem is considering the connection to the finger and the relative placement of the pockets carefully. This could lead to innovating a geometry that could theoretically enable abduction-adduction motion without causing simultaneous flexion.

### 5.2.2. Opposing Side-Pockets

Although Opposing-C's structure had several advantages considering both the flexion and abduction-adduction motions, it relied on a relatively large deformation of the opposing pockets to reach the target motions. This led to a clear change in response and made the actuator unreliable and potentially unsafe. Furthermore, the opposing pockets' deformation was not equal (Figure 10), which was caused by inaccurate fabrication methods leading to uneven silicone thickness in functionally critical parts. These aspects make the approach the most difficult to develop into a working design for this application, as it would require radical changes to the geometry and materials.

These problems could be solved by embedding additional reinforcing materials inside the elastomer parts that press against each other, to make them more robust, similar to the work of Shepherd et al. [36]. Furthermore, making the gap between the pockets smaller would minimize the required deformation to reach large enough displacements of the joint.

On the other hand, the pockets could be designed to be more like bellows that fold on themselves when deflated and unfold when inflated, similar to the actuators by Belforte et al. [7] or by Galloway et al. [30]. Using this kind of pleat would reduce the amount of deformation required from individual parts of the structure to reach a large bending motion. This, however, could decrease the

resulting curvature or make the abduction-adduction motion less like that of a pivot joint, which we see as one of the main strengths of the studied design.

### 5.2.3. Parallel Pockets

The main disadvantage of the parallel pocket design was related to its excessive lengthwise expansion, which caused, e.g., unwanted deformation of the actuator under the connecting straps. This could be reduced by making the pockets shorter so that they would be more localized on top of the joint. On the other hand, a longer than necessary pocket structure could be utilized by localizing the deformation by using stiffer restricting sleeves, following the example of Galloway et al. [25]. This way, the actuators could be adjusted, to some degree, for different hand sizes.

Another difficulty in this design is the required fabrication precision, as the actuator needs to be as symmetrical as possible to allow for symmetrical output. Although we did our best to make the prototype as symmetrical as possible, a slight deviation from the wanted trajectory and some difference in torque in each direction can still be seen in the results. This could be mitigated by making the pockets shorter and also improving the fabrication methods.

One way of amplifying the four pockets' directional control would be to include a supporting, flexible, but much less extensible spine in the middle of the actuator. This spine would consist of, or envelop, the input tubing for the actuator structure's distal pockets that control the flexion of the finger's IP joints.

The amount of separately-controlled pockets is also problematic. Although this time, we tested a four-pocket design, it may be possible to simplify it to be effective with only three pockets. This would be advantageous, as the amount of inputs would be reduced by five for a full glove, making the design equal to the simple side-pocket prototypes with regard to required inputs.

## 5.3. Future Work

In the future, we will continue the development of our actuators' MCP part mainly based on the parallel pocket design, as we see it to have the most potential to be applied in a full power-assist glove for rehabilitation. In addition, we believe this design could be applied to thumb motions relatively easily, by adjusting its pocket sizes for controlling the motions of the carpometacarpal joint. Next, we will add IP joint flexion to have control over all of the finger joints and then scale the actuator to fit each finger. These actuators are then combined into a full motion-assist glove, which is tested for its ability in achieving the target six-pack motions. The actuators' function will be tested first on an improved dummy finger system. After this, we will move on to tests on human subjects and clinical trials on actual patients, to determine the actuators' and glove system's effectiveness on real hands.

In this study, we did not test Parallel-D's controllability with differential pressures in depth, as our goal was to find the differences between the three approaches and compare their potential for full MCP joint motion support. However, we will be studying the differential control further, as it is crucial to confirm its usability in practice, especially when connected to a finger.

One of the most usual comments from therapists has been that the actuators should also enable active extension of the coupled digits. This way, the developed glove would be useful for most patients, as one of the prevalent effects of hand disabilities is the involuntary flexion of the digits. This leads to a claw-like posture of the hand. Thus, in the future, we will also be considering the implementation of extension as an active mode of actuation in our device.

Another commonly-mentioned feature in discussions with therapists is at-home rehabilitation. This would improve the accessibility of the exercises, as the patient would not need to go to the clinic to receive therapy. Thus, we aim to make the system portable, easy to use by non-professionals and inexpensive.

## 6. Conclusions

The aim of this study was to explore the development of soft fiber-reinforced actuators for 2-DoF assist (abduction-adduction and flexion) of the MCP joint. So far, the combination of these motions has not been implemented in soft rehabilitation gloves, which limits the possible exercises that can be done with them. We believe that one of the main reasons for this is the difficulty of separating the two functions of the same soft structure so that they do not get coupled and have detrimental effects on each other.

We presented three different approaches to making multi-pocket actuators for controlling the two DoFs separately and evaluated their feasibility. Two of them (simple side-pockets and opposing pockets) were targeted specifically for the MCP joint and had control only in the direction of the joint's two motion axes. The third one (parallel pockets) was designed to allow a full 360° control of the actuator motion through differential pressures. We produced five prototypes, which we tested in torque and trajectory measurements.

Each of the approaches had advantages and disadvantages over the others, and we presented our analysis on how they could be improved to make each one work.

Our results can be used to expand the variety of achievable functions with soft fiber-reinforced actuators. Thus, we have taken a step closer to full motion assist of the human body with soft, safe, inexpensive and comfortable wearable robotics.

**Supplementary Materials:** Supplementary materials include all the used measurement data, and photos of the prototypes and motion capture/torque measurements are available online at <http://www.mdpi.com/2076-0825/6/3/27/s1>.

**Acknowledgments:** We would like to thank Masashi Sekine, Jiang Wu and Kouki Shiota for technical support in the project. Kouki Shiota contributed to the preparation of Figure 2. We would also like to thank Jacobo Fernandez-Vargas and Kornkanok Tripanpitak for their comments on the manuscript. Kornkanok Tripanpitak provided also invaluable insight to physical therapy. This work was supported by JSPS Grant-in-Aid for Scientific Research (B) 17H02129.

**Author Contributions:** Tapio Veli Juhani Tarvainen was the main author of the manuscript and conducted the design, fabrication and testing of the presented prototypes. Wenwei Yu was the main supervisor and advisor of the work and contributed to the manuscript by reviewing and revising its contents.

**Conflicts of Interest:** The authors declare no conflict of interest. The funding sponsors had no role in the design of the study; in the collection, analyses or interpretation of data; in the writing of the manuscript; nor in the decision to publish the results.

## Abbreviations

The following abbreviations are used in this manuscript:

MCP	Metacarpophalangeal (joint)
IP	Interphalangeal (joint)
DoA	Degree of Actuation
DoF	Degree of Freedom

## References

1. Heo, P.; Gu, G.M.; Lee, S.J.; Rhee, K.; Kim, J. Current hand exoskeleton technologies for rehabilitation and assistive engineering. *Int. J. Precis. Eng. Manuf.* **2012**, *13*, 807–824.
2. Lum, P.S.; Godfrey, S.B.; Brokaw, E.B.; Holley, R.J.; Nichols, D. Robotic approaches for rehabilitation of hand function after stroke. *Am. J. Phys. Med. Rehabil.* **2012**, *91*, S242–S254.
3. Maciejasz, P.; Eschweiler, J.; Gerlach-Hahn, K.; Jansen-Troy, A.; Leonhardt, S. A survey on robotic devices for upper limb rehabilitation. *J. NeuroEng. Rehabil.* **2014**, *11*, doi:10.1186/1743-0003-11-3.
4. Volpe, B.T.; Ferraro, M.; Lynch, D.; Christos, P.; Krol, J.; Trudell, C.; Krebs, H.I.; Hogan, N. Robotics and other devices in the treatment of patients recovering from stroke. *Curr. Neurol. Neurosci. Rep.* **2005**, *5*, 465–470.
5. Abidi, H.; Cianchetti, M. On intrinsic safety of soft robots. *Front. Robot. AI* **2017**, *4*, doi:10.3389/frobt.2017.00005.
6. Rus, D.; Tolley, M.T. Design, fabrication and control of soft robots. *Nature* **2015**, *521*, 467–475.

7. Belforte, G.; Eula, G.; Ivanov, A.; Sirolli, S. Soft pneumatic actuators for rehabilitation. *Actuators* **2014**, *3*, 84–106.
8. Kang, B.B.; Lee, H.; In, H.; Jeong, U.; Chung, J.; Cho, K.J. Development of a polymer-based tendon-driven wearable robotic hand. In Proceedings of the IEEE International Conference on Robotics and Automation (ICRA), Stockholm, Sweden, 16–21 May 2016; pp. 3750–3755.
9. Park, Y.L.; Santos, J.; Galloway, K.G.; Goldfield, E.C.; Wood, R.J. A soft wearable robotic device for active knee motions using flat pneumatic artificial muscles. In Proceedings of the 2014 IEEE International Conference on Robotics and Automation (ICRA), Hong Kong, China, 31 May–7 June 2014; pp. 4805–4810.
10. Zhao, H.; Li, Y.; Elsamadisi, A.; Shepherd, R. Scalable manufacturing of high force wearable soft actuators. *Extreme Mech. Lett.* **2015**, *3*, 89–104.
11. Moore, H.; Nichols, C.; Engles, M.L. *Orthopaedic Physical Therapy*; Churchill Livingstone: New York, NY, USA, 2009; Chapter 1, pp. 16–20.
12. Noritsugu, T.; Takaiwa, M.; Sasaki, D. Power assist wear driven with pneumatic rubber artificial muscles. In Proceedings of the 15th International Conference on Mechatronics and Machine Vision in Practice, Auckland, New Zealand, 2–4 December, 2008; pp. 539–544.
13. Polygerinos, P.; Wang, Z.; Galloway, K.C.; Wood, R.J.; Walsh, C.J. Soft robotic glove for combined assistance and at-home rehabilitation. *Robot. Auton. Syst.* **2015**, *73*, 135–143.
14. Yap, H.K.; Khin, P.M.; Koh, T.H.; Sun, Y.; Liang, X.; Lim, J.H.; Yeow, C.H. A fully fabric-based bidirectional soft robotic glove for assistance and rehabilitation of hand impaired patients. *IEEE Robot. Autom. Lett.* **2017**, *2*, 1383–1390.
15. Gerboni, G.; Ranzani, T.; Diodato, A.; Ciuti, G.; Cianchetti, M.; Menciassi, A. Modular soft mechatronic manipulator for minimally invasive surgery (MIS): Overall architecture and development of a fully integrated soft module. *Mecanica* **2015**, *50*, 2865–2878.
16. Deimel, R.; Brock, O. A novel type of compliant and underactuated robotic hand for dexterous grasping. *Int. J. Robot. Res.* **2016**, *35*, 161–185.
17. Yap, H.K.; Lim, J.H.; Nasrallah, F.; Goh, J.C.H.; Yeow, C.H. A soft exoskeleton for hand assistive and rehabilitation application using pneumatic actuators with variable stiffness. In Proceedings of the 2015 IEEE International Conference on Robotics and Automation (ICRA), Seattle, WA, USA, 26–30 May 2015, pp. 4967–4972.
18. Tarvainen, T.V.J.; Yu, W. Preliminary results on multi-pocket pneumatic elastomer actuators for human–robot interface in hand rehabilitation. In Proceedings of the 2015 IEEE International Conference on Robotics and Biomimetics (ROBIO), Zhuhai, China, 6–9 December 2015; pp. 2635–2639.
19. Howell, L.L. *Compliant Mechanisms*; John Wiley & Sons: New York, NY, USA, 2001.
20. Polygerinos, P.; Wang, Z.; Overvelde, J.T.B.; Galloway, K.C.; Wood, R.J.; Bertoldi, K.; Walsh, C.J. Modeling of soft fiber-reinforced bending actuators. *IEEE Trans. Robot.* **2015**, *31*, 778–789.
21. Udupa, G.; Sreedharan, P.; Dinesh, P.S.; Kim, D. Asymmetric bellow flexible pneumatic actuator for miniature robotic soft gripper. *J. Robot.* **2014**, *2014*, doi:10.1155/2014/902625.
22. Connolly, F.; Walsh, C.J.; Bertoldi, K. Automatic design of fiber-reinforced soft actuators for trajectory matching. *Proc. Nat. Acad. Sci. USA* **2017**, *114*, 51–56.
23. Connolly, F.; Polygerinos, P.; Walsh, C.J.; Bertoldi, K. Mechanical programming of soft actuators by varying fiber angle. *Soft Robot.* **2015**, *2*, 26–32.
24. Bishop-Moser, J.; Krishnan, G.; Kim, C.; Kota, S. Design of soft robotic actuators using fluid-filled fiber-reinforced elastomeric enclosures in parallel combinations. In Proceedings of the IEEE/RSJ International Conference on Intelligent Robots and Systems (IROS), Vilamoura, Portugal, 7–12 October 2012; pp. 4264–4269.
25. Galloway, K.C.; Polygerinos, P.; Walsh, C.J.; Wood, R.J. Mechanically programmable bend radius for fiber-reinforced soft actuators. In Proceedings of the 16th International Conference on Advanced Robotics (ICAR), Montevideo, Uruguay, 25–29 November 2013; pp. 1–6.
26. Hume, M.C.; Gellman, H.; McKellop, H.; Brumfield, R.H., Jr. Functional range of motion of the joints of the hand. *J. Hand Surg.* **1990**, *15*, 240–243.
27. Bishop, H.J.; Montgomery, J. *Daniels and Worthingham's Muscle Testing*, 8th ed.; Saunders Elsevier: St. Louis, MO, USA, 2007.

28. Kawasaki, H.; Kimura, H.; Ito, S.; Nishimoto, Y.; Hayashi, H.; Sakaeda. Hand rehabilitation support system based on self-motion control, with a clinical case report. In Proceedings of the 2006 World Automation Congress, Budapest, Hungary, 24–26 July 2006; pp. 1–6.
29. Buryanov, A.; Kotiuk, V. Proportions of hand segments. *Int. J. Morphol.* **2010**, *28*, 755–758.
30. Galloway, K.C.; Becker, K.P.; Phillips, B.; Kirby, J.; Licht, S.; Tchernov, D.; Wood, R.J.; Gruber, D.F. Soft robotic grippers for biological sampling on deep reefs. *Soft Robot.* **2016**, *3*, 23–33.
31. Marchese, A.D.; Katzschmann, R.K.; Rus, D. A recipe for soft fluidic elastomer robots. *Soft Robot.* **2015**, *2*, 7–25.
32. Thingiverse. Available online: <http://www.thingiverse.com/> (accessed on 14 March 2017).
33. Ueki, S.; Kawasaki, H.; Ito, S.; Nishimoto, Y.; Abe, M.; Aoki, T.; Ishigure, Y.; Ojika, T.; Mouri, T. Development of a hand-assist robot with multi-degrees-of-freedom for rehabilitation therapy. *IEEE/ASME Trans. Mechatron.* **2012**, *17*, 136–146.
34. Cianchetti, M.; Ranzani, T.; Gerboni, G.; Falco, I.D.; Laschi, C.; Menciassi, A. STIFF-FLOP surgical manipulator: Mechanical design and experimental characterization of the single module. In Proceedings of the IEEE/RSJ International Conference on Intelligent Robots and Systems (IROS), Tokyo, Japan, 3–7 November 2013; pp. 3576–3581.
35. Wall, V.; Deimel, R.; Brock, O. Selective stiffening of soft actuators based on jamming. In Proceedings of the 2015 IEEE International Conference on Robotics and Automation (ICRA), Seattle, WA, USA, 26–30 May 2015; pp. 252–257.
36. Shepherd, R.F.; Stokes, A.A.; Nunes, R.M.D.; Whitesides, G.M. Soft machines that are resistant to puncture and that self seal. *Adv. Mater.* **2013**, *25*, 6709–6713.



© 2017 by the authors. Licensee MDPI, Basel, Switzerland. This article is an open access article distributed under the terms and conditions of the Creative Commons Attribution (CC BY) license (<http://creativecommons.org/licenses/by/4.0/>).